Impact of Land Use Land Cover Change on Land Surface Temperature Of Noida,India

Gaurav Pandey[*], Harsh Sahlot[*], Ayush Gautam[*] , Ashish Kumar[*],Abhishek Kumar[*]

[*]Undergraduate Scholars, Department of Civil Engineering, KIET Group of Institutions, Delhi-NCR, Ghaziabad

Abstract- Urbanisation is significantly influenced by land use and land cover change (LULCC), which has an impact on both society and the environment. In this study, we use Landsat 8/9 satellite data for 2013, 2018, and 2023 to investigate the effects of LULCC on land surface temperature (LST) in Noida, India (along with areas of Dadri). Classification has been done on the land cover classes and extracted LST values from the data using ArcGIS Pro software version 3.1.1.

In this study, we investigate the link between LST and LULCC has been investigated in Noida, with a particular emphasis on the impact of urbanisation on land surface temperature. The findings provide light on the temporal and geographical dynamics of LST and land cover types during the past ten years. We have been addressed the effects of these adjustments on urban planning and environmental management, with emphasis on the necessity for sustainable development approaches that strike a balance between urban expansion and resource preservation.

This study also illustrates about application of remote sensing and GIS technology may be used to track and examine LULCC and its environmental effects. This is a thorough study of the link between land cover types, surface temperature, and urbanisation in Noida using satellite data and GIS technologies. This work might guide future research and decision-making procedures concerning urban growth and environmental management.

Index Terms- Land use and land cover change (LULCC),Landsat 8/9, Spatial analysis, Temporal analysis, Image classification.

I. INTRODUCTION

Thermal characteristics of the Earth's surface have been significantly altered by the rapid speed of urbanisation and related land useand land cover change (LULCC), which has changed the land surface temperature (LST). Remote sensing and geographic information system (GIS) techniques have developed into effective tools for analysing the effects of LULCC on LST inrecent years. The current study uses Landsat 8/9 data and ArcGIS Pro software to examine the effects of LULCC on LST in Noida,

India. Due to urbanisation, Noida, a city in India's National Capital Region that is quickly growing, has seen substantial changes in its land use and land cover.

By examining changes in land use and land cover, we compare the LST of Noida for the years 2013, 2018, and 2023 in this study. Understanding LULCC's spatial and temporal patterns and how they affect LST is the main goal of the study. Environmental managers and politicians may utilise the study's findings to create sustainable urbanisation plans that strike a balance between economic growth and environmental preservation.

II. STUDY AREA AND DATA USED

NOIDA A planned, integrated, modern industrial city that is well connected to Delhi by a network of roads, national highways and the ultra-modern DND flyover, offering inter-road linkages to all parts of the country, NOIDA was established under the U.P. Industrial Area Development Act, 1976. NOIDA (along with DADRI included in this study), which spans 61188.1425 hectares or 611.881425 Km^2 and has several completely developed sectors, offers a pollution-free high level of life and a highly supportive industrial environment thanks to its distinctive infrastructure, which offers a multitude of unrivalled advantages. Today, it serves as an admirable example of an integrated industrial township, complete with wide, smooth roads, well-developed land, dependable power and telephone service, magnificent residential complexes, and an environment that is calm and peaceful with plenty of greenery.

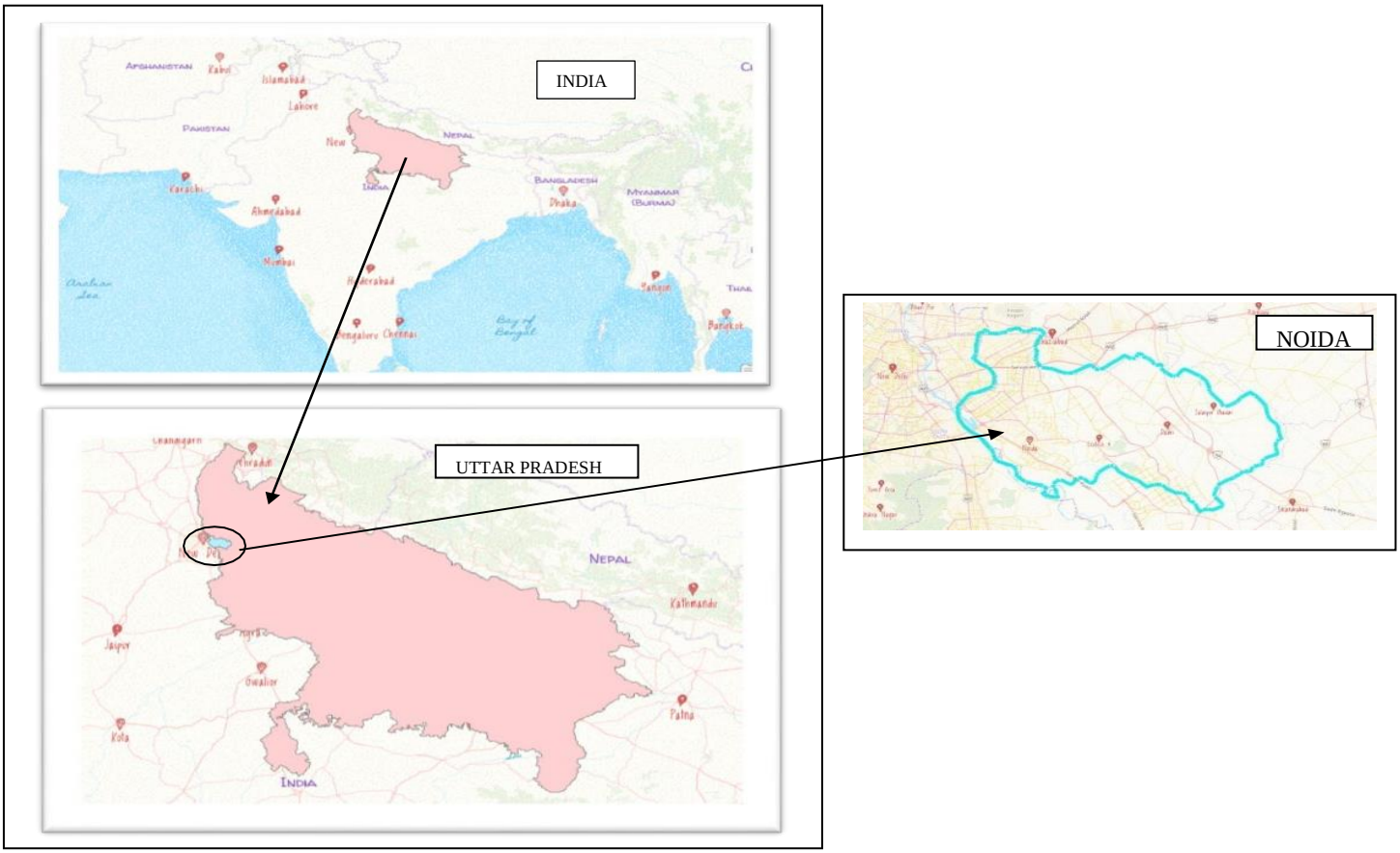

Figure 1. The study area of Noida, India.

Date Of acquisition	Platform	Sensor	Path/Row	Application
20 Oct 2013	Landsat 8	OLI/ TIRS	146/40	Classification, LST, Indices
02 Oct 2018	Landsat 8	OLI/TIRS	146/40	Classification, LST, Indices
23 Feb 2023	Landsat 9	OLI/TIRS	146/40	Classification, LST, Indices

Table 1. Description of Landsat satellite data used.

Landsat images used were acquired using different sensors viz. TM, ETM+ and OLI/TIRS for different dates (Table 1). Total 3 multi-sensor Landsat images have been used in this study for LULC classification, computation of various spectral indices and LST estimation. The spatial resolution of the imagery is 30 meters, except for the panchromatic band which has a resolution of 15 meters. In order to get the shapefile designated for NOIDA boundaries, we used GADM. The Global Aviation Data Management (GADM) program is a data management platform which integrates multiple sources of operational data received from various channels. GADM provides maps and spatial data for all countries and their sub-divisions. For the NOIDA REGION, we utilized the GADM_IND41 shape file with the FID - 2128 third level border distribution.

III. METHODOLOGY

The following literature provides a full breakdown of the processes involved in the planned study.

A. FOR LULCC ANALYSIS:

1) Preprocessing of Landsat 8 data: Atmospheric correction, radiometric calibration, and geometric correction of Landsat 8 data were performed using appropriate tools in ArcGIS Pro like :

Atmospheric Correction: The Atmospheric Correction tool in ArcGIS Pro can be used to remove the effects of atmospheric haze from the Landsat 8 imagery.

Radiometric Calibration: The Radiometric Calibration tool in ArcGIS Pro can be used to adjust the digital number (DN) values of the Landsat 8 imagery to radiance values.

2) Pan sharpening tool: The spatial resolution of the classified image was enhanced using the "Pan sharpening" tool in ArcGIS Pro. The high-resolution panchromatic band (Band – 8 in LANDSAT8/9) was fused with the multispectral bands using Gram-Schmidt method, and appropriate parameters were selected.

3) Composite band creation: The bands were stacked to create a composite band using the "Composite Bands" tool in ArcGIS Pro. The Composite Bands tool in ArcGIS Pro allows to create a composite image from two or more input bands. This tool combines the input bands into a single, multiband image that can be used for analysis, visualization, and interpretation. Composite bands can be created by combining different spectral bands from a Landsat 8 image. For example, one can create a composite image using the red, green, and blue bands of the Landsat 8 imagery. This type of composite is commonly used for visual interpretation and display.

There are different types of composite images that can be created using different band combinations. Here are some common types of composite images:

True Color Composite: Combines red, green, and blue bands to create an image that closely resembles what the human eye sees.

False Color Composite: Combines bands that are outside the visible spectrum, such as near-infrared, red, and green, to create an image that can highlight vegetation, soil moisture, and other features.

Color Infrared Composite: Combines near-infrared, red, and green bands to create an image that shows vegetation in shades of red.

4) Extraction of the study area: The area of interest was extracted by applying a mask to the

composite band using the "Extract by Mask" tool in ArcGIS Pro.

5) Classification based on pixels: The k-NN algorithm was applied for pixel-based classification using the "Train ISO Cluster" tool in ArcGIS Pro. A specific number of neighbors (500 in this study) were used, and the criteria used for assigning each pixel to a specific land cover class were based on spectral signatures and visual interpretation.

6) Validation of classification results: The accuracy of the classification results was validated using ground-truth data, a confusion matrix, and an overall accuracy assessment using the "Accuracy Assessment" tool in ArcGIS Pro.

Figure 3 depicts the methodology for LULC retrieval from spectral bands of LANDSAT 8/9.

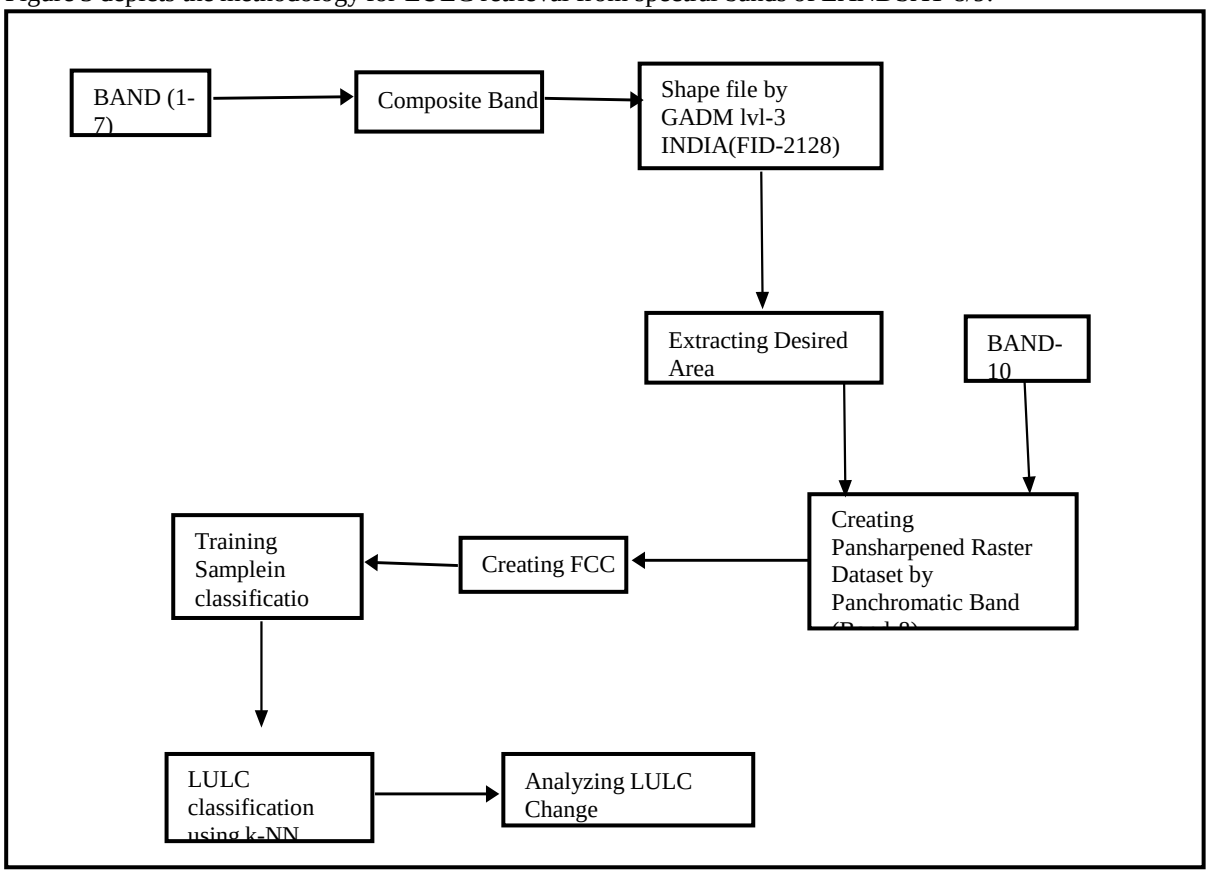

Figure 2 – Methodology for LULCC analysis

Band Designations	**Wavelength (μm)**	**Resolution (m)**
Band 1 (Coastal Aerosol)	0.43 - 0.45	30
Band 2 (Blue)	0.45 - 0.51	30
Band 3 (Green)	0.53 - 0.59	30
Band 4 (Red)	0.64 - 0.67	30
Band 5 (Infrared)	0.85 - 0.88	30
Band 6 (Short wave infrared)	1.57 - 1.65	30
Band 7 (Short wave infrared)	2.11 - 2.29	30
Band 8 (Panchromatic)	0.50 - 0.68	15
Band 9 (Cirrus)	1.36 - 1.39	30
Band 10 (Thermal infrared)	10.6 - 11.19	100
Band 11 (Thermal infrared)	11.50 - 12.51	100

Table 2. LANDSAT 8/9 OLI and TIRS

B. FOR LST ANALYSIS:

1) In Table 2, the satellite picture information is displayed. The initial phase of the proposed approach is to use the following equation to convert the band 10 DN (Digital Number) data to at-sensor spectral radiance.

$$L_\lambda = M_L * Q_{cal} + A_L - O_L$$

Where ,

Lλ -spectral radiance value

Qcal - quantized calibrated pixel value in DN

ML - radiance multiplicative scaling factor for the band,

AL - radiance additive scaling factor for the band

OL - correction for Band 10

2) The TIRS band data should be converted to brightness temperature (BT) using the thermal constants provided in the metadata file and the following equation after DN values have been converted to at-sensor spectral radiance.

$$BT = \frac{K2}{\ln\left[\left(\frac{K_1}{L\lambda}\right)+1\right]} - 273.15$$

Where ,

K1 and K2 are the thermal constants of TIR band 10 which can be identified in the metadata file associated with the satellite image.

Variable	Description	Value
K_1 K_2	Thermal constants, Band 10	774.8853 1321.0789
L_{max} L_{min}	Maximum and Minimum values of Radiance, Band 10	22.00180 0.10033
Q_{calmax} Q_{calmin}	Maximum and Minimum values of Quantize Calibration, Band 10	65535 1
O_i	Correction value, Band 10	0.29

Table 3. Metadata of the satellite image

3) To distinguish between the various land cover types in the research region, the Normalised Difference Vegetation Index (NDVI) is crucial. The NDVI scale goes from -1.0 to +1.0. The normalised difference between the near infrared band (0.85-0.88 m) and the red band (0.64- 0.67 m) of the pictures is used to compute NDVI on a per-pixel basis using the equation :

$$NDVI = \frac{(NIR-RED)}{(NIR+RED)}$$

Where ,

NIR - near infrared band value of a pixel

RED - red band value of the same pixel.

For Landsat 8/9 :

Band 5 – NIR,

Band 4 – RED

4) The following step is to use the NDVI data acquired in step 3 to determine proportional vegetation (Pv). This proportional vegetation provides an estimate of the area covered by each kind of land cover. The proportions of vegetation and bare soil are obtained from the NDVI of clean pixels. P_v can be calculated using the equation:

$$P_v = \left(\frac{NDVI-NDVI_s}{NDVI_v-NDVI_s}\right)^2$$

5) Since land surface emissivity (LSE) is a proportionality factor that scales the black body radiance (Plank's law) to measure emitted radiance and it is the capacity of transporting thermal energy over the surface into the atmosphere [10], it must be calculated in order to estimate LST. Natural surfaces are

$$\varepsilon_\lambda = \varepsilon_{v\lambda} P_v + \varepsilon_{s\lambda} (1 - P_v) + C_\lambda$$

diverse in terms of LSE variation at the pixel level. The LSE also heavily depends on factors like plant

type, surface roughness, and others. It can be calculated by given equation:

Where:

εv - vegetation emissivity

εs - soil emissivity

C - surface roughness taken as a constant value of 0.005

When the NDVI is less than 0, the land cover type is classified as water, and the emissivity value of 0.991 is given. When the NDVI is between 0 and 0.2, the land cover type is considered to be soil, and the emissivity value of 0.966 is assigned. When the NDVI is between 0.2 and 0.5, the land cover type is considered to be a mixture of soil and vegetation cover, and above equation is used to calculate the emissivity. In the final scenario, plant cover is assumed when the NDVI value is larger than 0.5, and a value of 0.973 is assigned.

6) The last procedure is to compute LST using LSE obtained from Pv and NDVI and brightness temperature (BT) of band 10.The following equation allows for the retrieval of LST:

$$T_s = \frac{BT}{\{1 + [(\lambda BT/\rho) ln\varepsilon_\lambda]\}}$$

Where,

Ts - LST in Celsius (^oC),

BT - at- sensor BT(^oC),

λ - average wavelength of band 10,

ελ - emissivity calculated from equation

ρ - 1.438 x 10-2 mK

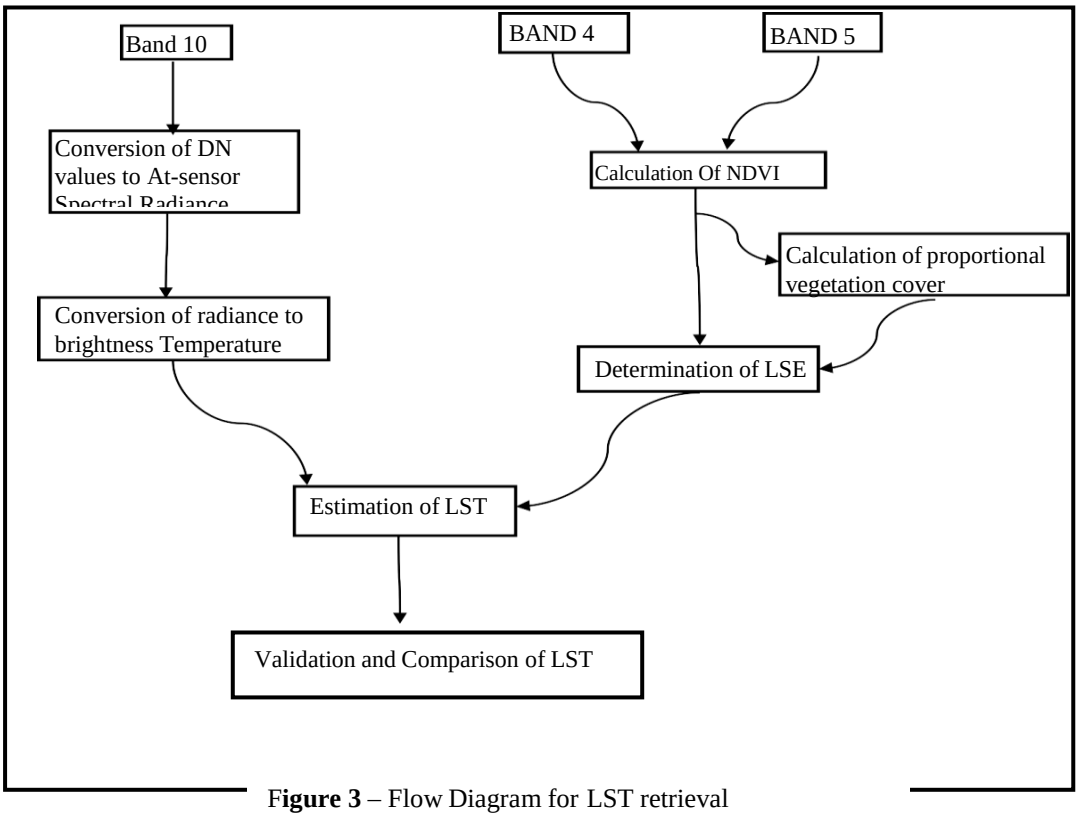

Figure 3 – Flow Diagram for LST retrieval

Figure 2 depicts the methodology for the planned effort to estimate LST. Data from LANDSAT 8/9 can only be processed using this method. Band 10 is utilized in this study to determine NDVI while band 4 and 5 are used to evaluate brightness temperature.

IV. RESULT AND ANALYSIS

The study area of Noida, India, is shown in Figure 1. Satellite images of three dates of same region were downloaded from USGS website. The study area chosen includes water, bare soil, vegetation cover and built-up area. Landsat 8/9 data for the dates 20/10/2013, 02/10/2018 and 23/02/2023 (path/row: 146/40) were used for the present study. The Visible bands and Near Infrared bands are combined together to form a False Color Composite (FCC) image. The images were resampled using kth nearest neighbor method. All the data were re-projected to a Universal Transverse Mercator (UTM) coordinate system, datum WGS84, zone 44. The FCC images were created by layer stacking band 4, band 3 and band 2 of each data set correspondingly.

Figure 4. NDVI images for (a) 20/10/2013, (b) 23/10/2018 and (c) 23/02/2023

Each dataset's NDVI is determined following the conversion of the DN values to spectral radiances. Figure 4 displays the NDVI pictures. When compared to the NDVI of 2013 and 2018, the NDVI for vegetated land covers will be better in 2023. That indicates that vegetation has grown, which has an effect on the surface temperature. However, the NDVI for land cover categories including built-up areas and barren terrain has not changed significantly. For the collected satellite data, LSE were predicted to recover LST.

The increasing urbanisation that is taking place in LULCC is evident. Both the amount of vegetation and the amount of bare land have significantly decreased. Figure 5 shows the LULC with various types of land cover, including flora, water, bare ground, and urbanisation.

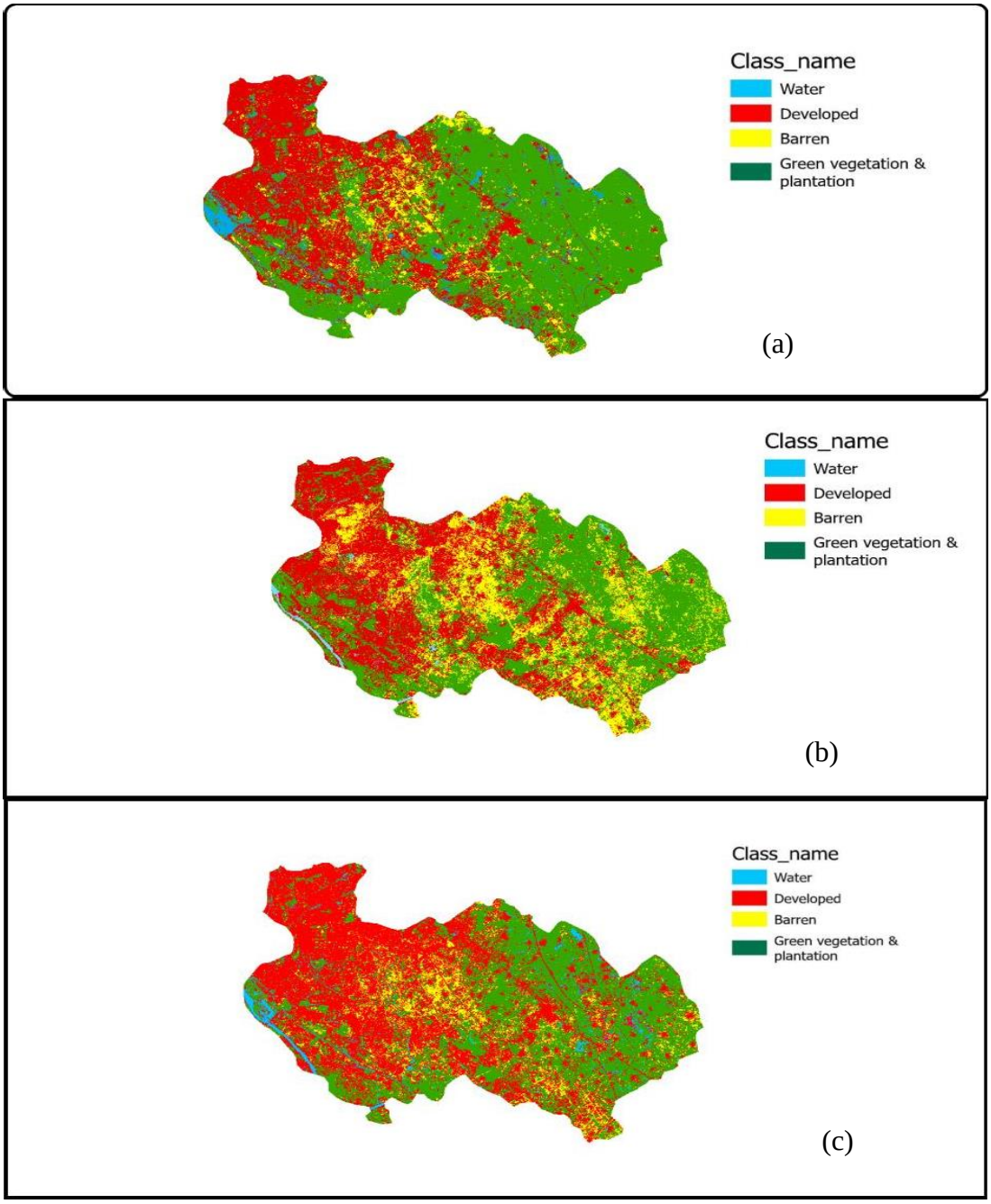

Figure 5. LULC for (a) 20/10/2013, (b) 23/10/2018 and (c) 23/02/2023

	OID *	Value	Classvalue	Class_name	Red	Green	Blue	Area
1	1	0	10	Water	84	117	168	22.201875
2	2	1	20	Developed	232	209	209	211.758475
3	3	2	30	Barren	210	205	192	47.3787
4	4	3	50	Green vegetation & pla...	170	255	0	330.542375

2013

	OID *	Value	Classvalue	Class_name	Red	Green	Blue	Area
1	1	0	10	Water	84	117	168	25.787025
2	2	1	20	Developed	232	209	209	237.5637
3	3	2	30	Barren	210	205	192	97.4715
4	4	3	50	Green vegetation & pla...	170	255	0	251.0592

2018

	OID *	Value	Classvalue	Class_name	Red	Green	Blue	Area
1	1	0	10	Water	84	117	168	21.20935
2	2	1	20	Developed	232	209	209	287.235975
3	3	2	30	Barren	210	205	192	55.597175
4	4	3	50	Green vegetation & pla...	170	255	0	247.838925

2023

Figure 6. Data of LULC for (a) 20/10/2013, (b) 23/10/2018 and (c) 23/02/2023

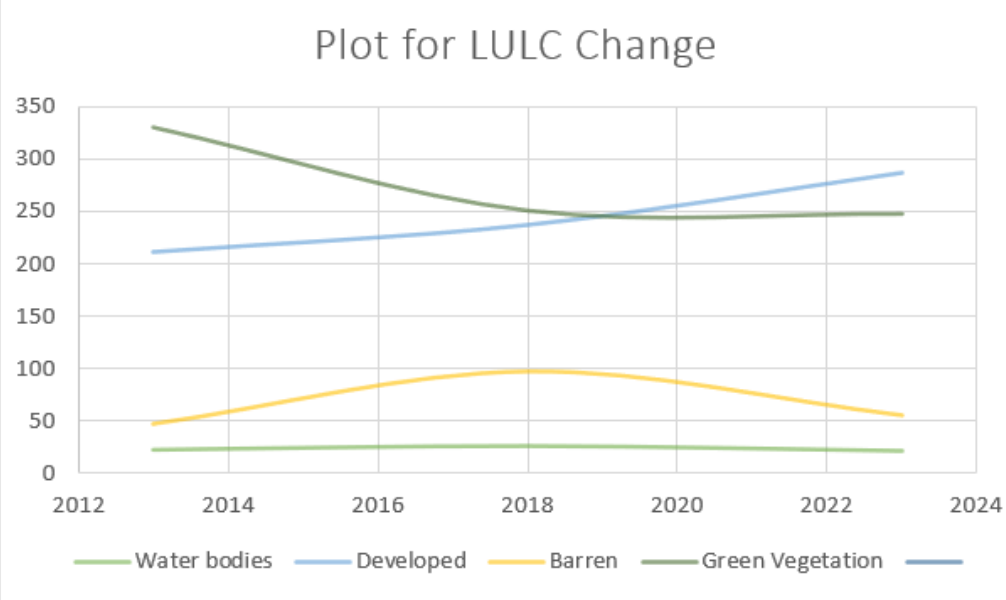

Figure 7 Time Series for LULC quantities

It can be shown that between 2013 and 2015, urbanisation increased by 10%, and between 2023 and 2015, it increas % increase can be observed from 2013 to 2018; however, it decreased to 43% from 2018 to 2023. In terms of vegetation, a 23% decline can be noted from 2013 to 2018; however, it further decreased to 1.58% from 2018 to 2023. The flow chart in figure 7 helps to further explain this facts.

While analysing LST it can be seen there is sudden change in temperatures in between 2013-2023.LST mentioned in figure 8 . it appears that there are significant changes in the land surface temperature (LST) of Noida over the study period of 2013-2023. The mean LST in 2013 was 28.72088°C, while in 2018 it increased to 30.47286°C, and in 2023 it decreased to 24.15437°C. The standard deviation of LST also varied across the study period, with the highest standard deviation in 2023 (1.96904°C) and the lowest standard deviation in 2013 (1.72232°C).

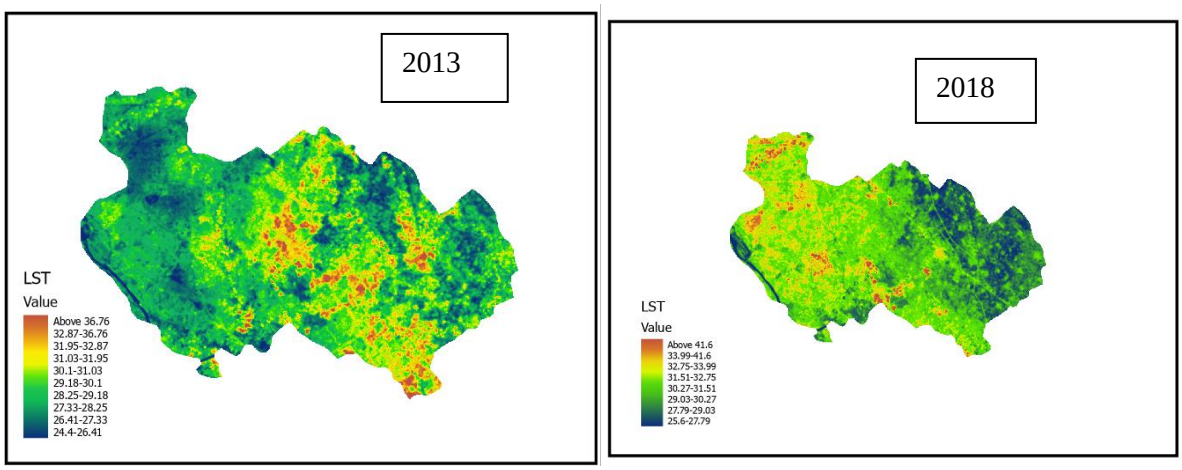

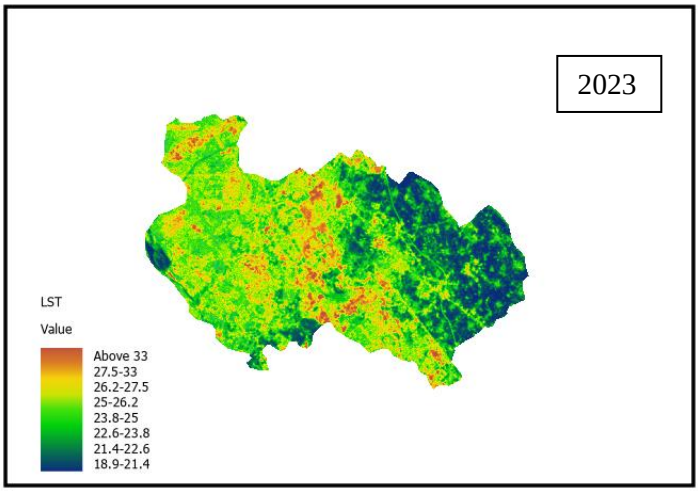

Figure.8 LST for (a) 20/10/2013, (b) 23/10/2018 and (c) 23/02/2023

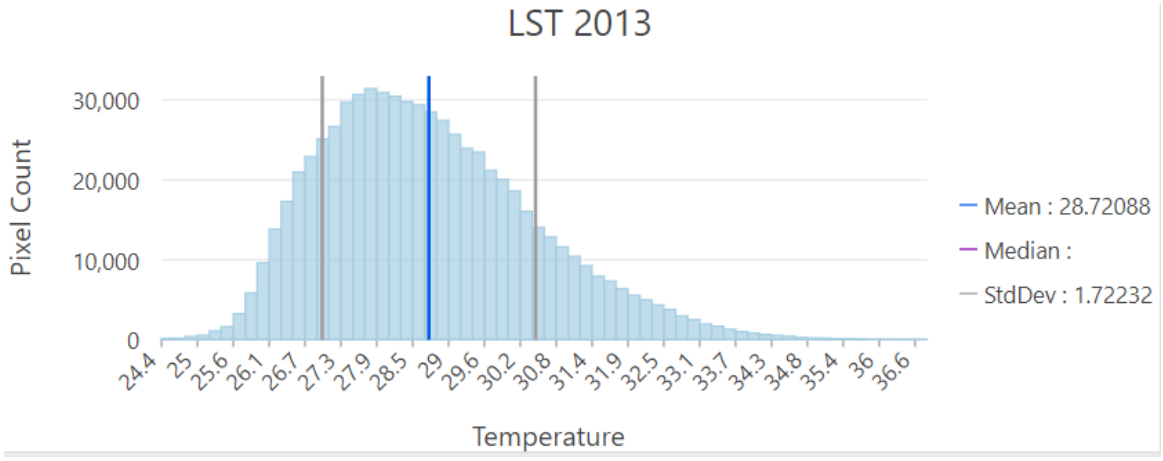

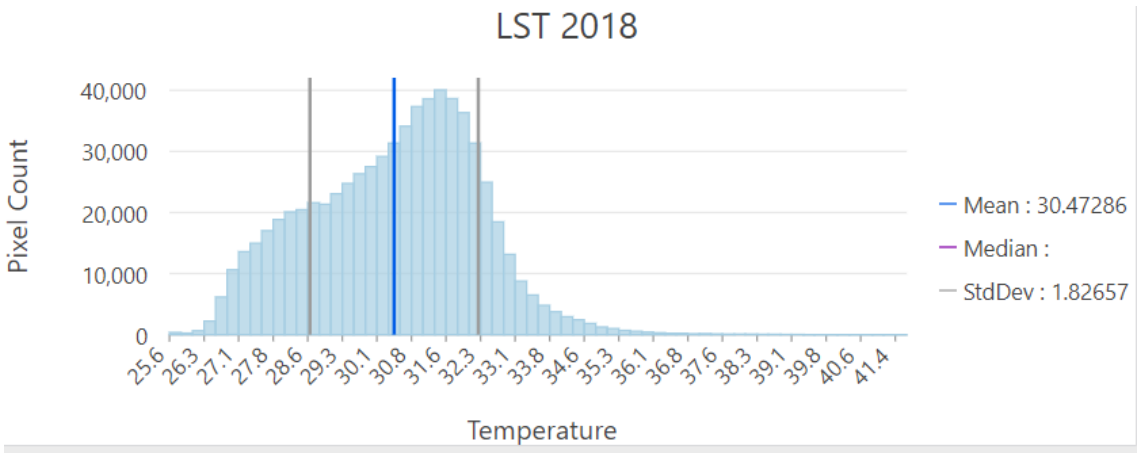

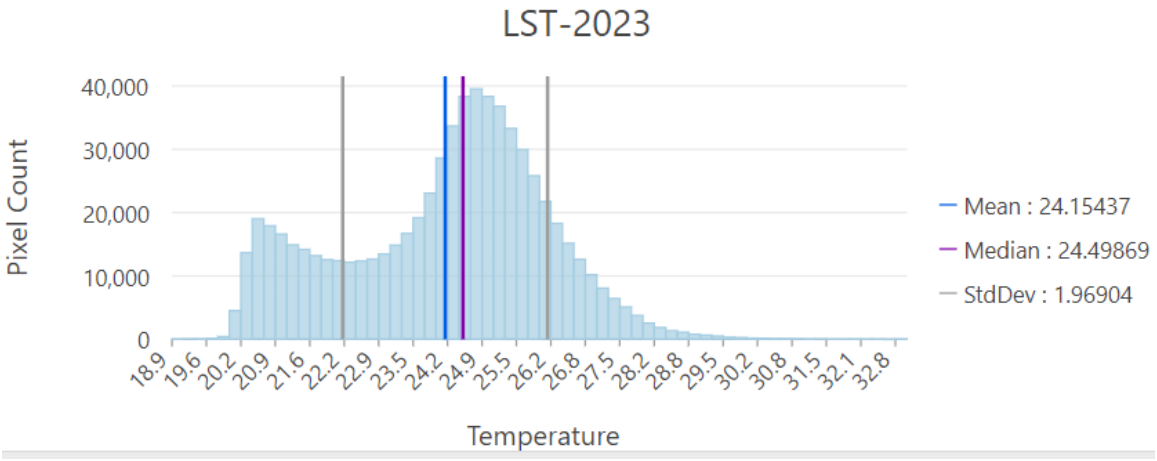

Figure 9. LST histogram analysis for (a) 20/10/2013, (b) 23/10/2018 and (c) 23/02/2023

These findings suggest that there has been a significant change in the temperature patterns of Noida over the years, with the highest temperature being recorded in 2018. The decrease in LST in 2023 could be due to a number of factors, such as changes in land use or weather patterns. The increase in standard deviation in 2023 indicates that there is a greater variation in LST across the study area.

Overall, these findings suggest that there is a need for further investigation into the factors driving these changes in LST in Noida, and what their potential impacts could be on the environment and human health.The results of the LST analysis have implications for urban planning and management in Noida. The increase in temperature can negatively affect human comfort, health, and productivity. It can also increase the energy demand for cooling and contribute to urbanheat island effects. Therefore, measures such as promoting green infrastructure and adopting cool roof technologies can be implemented to mitigate the effects of urbanization on LST and improve the overall urban environment.

Overall, the analysis of LST in Noida over a 10-year period highlights the importance of monitoring changes in land use and implementing sustainable urban planning strategies to mitigate the effects of urbanization on the environment and human well-being.

V. CONCLUSION

Our study investigated the impact of land use land cover change on normalized land surface temperature (LST) in Noida, India, using Landsat 8 and 9 data. The results of our analysis showed that there were significant changes in both LULC and LST over the period of 2013-2023. The LULC classification showed an increase in urbanization and decrease in vegetation cover, which was also reflected in the LST analysis. The findings suggest that land use change has a significant impact on surface temperature in urban areas, with urbanization leading to increased surface temperature.

The study utilized various tools and techniques, such as composite bands, pansharpening, and k-NN classification, to process and analyze the data. These tools and techniques proved to be effective in extracting relevant information from the Landsat data, allowing for a detailed analysis of LULC change and its impact on surface temperature.

Overall, the study provides valuable insights into the relationship between land use land cover change and surface temperature in urban areas, and highlights the importance of careful management of urbanization and green spaces to mitigate the urban heat island effect. The findings of this study have important implications for urban planners, policymakers, and researchers working on issues related to climate change and urban sustainability.

VI. ACKNOWLEDGMENT

Authors acknowledge Unites States Geological Survey for data used in the present study. Authors are thankful to the anonymous reviewers for providing their invaluable inputs to improve this manuscript.

VII. DISCLOSURE STATEMENT

No potential conflict of interest was reported by the author(s).

VIII. REFERENCES

1. Alrababah MA, Alhamad MN. 2006. Land use/cover classification of arid and semi-arid Mediterranean landscapes using Landsat ETM. Int J Remote Sens. 27(13):2703–2718.
2. Anderson JR. 1976. A land use and land cover classification system for use with remote sensor data (U.S. Geological Survey professional paper; 964). Washington: US Government Printing Office.
3. Avdan U, Jovanovska G. 2016. Algorithm for automated mapping of land surface temperature using LANDSAT 8 satellite data. J Sens. 2016:1–8.
4. Baig MHA, Zhang L, Shuai T, Tong Q. 2014. Derivation of a tasselled cap transformation based on Landsat 8 at-satellite reflectance. Remote Sens Lett. 5(5):423–431.
5. Bakr N, Weindorf DC, Bahnassy MH, Marei SM, El-Badawi MM. 2010. Monitoring land cover changes in a newly reclaimed area of Egypt using multi-temporal Landsat data. Appl Geogr. 30(4):592–605.
6. Chavez PS, Berlin GL, Sowers LB. 1982. Statistical method for selecting landsat MSS. J Appl Photogr Eng. 8(1):23–30.
7. Chen J, Gong P, He C, Pu R, Shi P. 2003. Land-use/land-cover change detection using improved changevector analysis. Photogramm Eng Remote Sens.69(4):369– 379.
8. Chowdhury M, Hasan ME, Abdullah-Al-Mamun MM. 2020. LZand use/land cover change assessment of Halda watershed using remote sensing and GIS. Egyptian J Remote Sens Space Sci. 23(1):63–75.
9. Clawson M, Stewart CL. 1965. Land use information. A critical survey of US statistics including possibilities for greater uniformity. Baltimore (MD): The Johns Hopkins Press.
10. Deng C, Wu C. 2012. BCI: a biophysical composition index for remote sensing of urban environments. Remote Sens Environ. 127:247–259.
11. Deng Y, Wu C, Li M, Chen R. 2015. RNDSI: a ratio normalized difference soil index for remote sensing of urban/suburban environments. Int J Appl Earth Obs Geoinf. 39:40–48.

12. Gangkofner UG, Pradhan PS, Holcomb DW. 2007. Optimizing the high-pass filter addition technique for image fusion. Photogramm Eng Remote Sens. 73(9):1107–1118.GEOCARTO INTERNATIONAL 21

13. Hislop S, Jones S, Soto-Berelov M, Skidmore A, Haywood A, Nguyen TH. 2018. Using Landsat spectral indices in time-series to assess wildfire disturbance and recovery. Remote Sens. 10(3):460.

14. Huang C, Wylie B, Yang L, Homer C, Zylstra G. 2002. Derivation of a tasselled cap transformation based on Landsat 7 at-satellite reflectance. Int J Remote Sens. 23(8):1741–1748.

15. Hussain A, Bhalla P, Palria S. 2014. Remote sensing based analysis of the role of land use/land cover on surface temperature and temporal changes in temperature; a case study of Ajmer District, Rajasthan.

16. The International Archives of Photogrammetry. Int Arch Photogramm Remote Sens Spatial Inf Sci. XL-8(8):1447–1454.

17. Jimenez-Munoz JC, Sobrino JA, Skokovi ~ c D, Mattar C, Crist obal J. 2014. Land surface temperature retrieval methods from Landsat-8 thermal IR sensor data. IEEE Geosci Remote Sens Lett. 11(10):1840–1843.

18. Kamini J, Jayanthi SC, Raghavswamy V. 2006. Spatio-temporal analysis of land use in urban Mumbaiusing multi-sensor satellite data and GIS techniques. J Ind Soc Remote Sens. 34(4):385–396.

19. Kendall MG. 1975. Rank correlation methods. London: Charles Griffin.Khatami R, Mountrakis G, Stehman SV. 2016. A meta-analysis of remote sensing research on supervisedpixel-based land-cover image classification processes: general guidelines for practitioners and future research. Remote Sens Environ. 177:89–100.

20. Kobayashi N, Tani H, Wang X, Sonobe R. 2020. Crop classification using spectral indices derived from Sentinel-2A imagery. J Inf Telecommun. 4(1):67–90.

21. Piyoosh AK, Ghosh SK. 2017. Semi-automatic mapping of anthropogenic impervious surfaces in an urban/suburban area using Landsat 8 satellite data. GISci Remote Sens. 54(4):471–494.

22. Piyoosh AK, Ghosh SK. 2018. Development of a modified bare soil and urban index for Landsat 8 satellite data. Geocarto Int. 33(4):423–442.

23. Qian L-X, Cui H-S, Chang J. 2006. Impacts of land use and cover change on land surface temperature in the Zhujiang Delta. Pedosphere. 16(6):681–689.

24. Rahman A, Kumar S, Fazal S, Siddiqui MA. 2012. Assessment of land use/land cover change in the North-West District of Delhi using remote sensing and GIS techniques. J Indian Soc Remote Sens. 40(4):689–697.

25. Rawat JS, Kumar M. 2015. Monitoring land use/cover change using remote sensing and GIS techniques: a case study of Hawalbagh block, district Almora, Uttarakhand, India. Egyptian J Remote Sens Space Sci. 18(1):77–84.

AUTHORS

Gaurav Pandey – Department of Civil Engineering, KIET Group of Institutions, Ghaziabad, India;

Harsh Sahlot – Department of Civil Engineering, KIET Group of Institutions, Ghaziabad, India;

Ayush Gautam – Department of Civil Engineering, KIET Group of Institutions, Ghaziabad, India;

Ashish Kumar – Department of Civil Engineering, KIET Group of Institutions, Ghaziabad, India;

Abhishek Kumar – Department of Civil Engineering, KIET Group of Institutions, Ghaziabad, India;